Ultrasound Obstet Gynecol 2012; **39**: 131–144
Published online 9 January 2012 in Wiley Online Library (wileyonlinelibrary.com). **DOI:** 10.1002/uog.9064

Functional assessment of the fetal heart: a review

M. E. GODFREY*, B. MESSING†, S. M. COHEN†, D. V. VALSKY† and S. YAGEL†

**Department of Pediatric Cardiology, Schneider Children's Medical Center Israel, Petach Tikva, Israel; †Department of Obstetrics and Gynecology, Hadassah-Hebrew University Medical Centers, Jerusalem, Israel*

KEYWORDS: 3DUS; 4DUS; E/A ratio; fetal heart; four-dimensional ultrasound; magnetic resonance imaging; M-mode; MPI; MRI; myocardial performance index; prenatal diagnosis; speckle tracking; strain rate; three-dimensional ultrasound; tissue Doppler

ABSTRACT

The purpose of this review is to evaluate the current modalities available for the assessment of fetal cardiac function. The unique anatomy and physiology of the fetal circulation are described, with reference to the difference between in-utero *and* ex-utero *life. M-mode, early/atrial ratio, myocardial performance index, three-dimensional and four-dimensional ultrasound, tissue Doppler including strain and strain rate, speckle tracking, magnetic resonance imaging and venous flow assessment are described. The modalities are analyzed from the perspective of the clinician and certain questions are posed. Does the modality assess systolic function, diastolic function or both? Is it applicable to both ventricles? Does it require extensive post-processing or additional hardware, or does it make use of technology already available to the average practitioner? The reproducibility and reliability of the techniques are evaluated, with reference to their utility in clinical decision-making. Finally, directions for future research are proposed. Copyright © 2012 ISUOG. Published by John Wiley & Sons, Ltd.*

INTRODUCTION

The purpose of this review is to analyze the current modalities available for the assessment of fetal cardiac function. The fetal heart differs from the *ex-utero* heart in both structure and function. The fetal heart represents two circulations, which effectively run in parallel, with two 'shunts' connecting them, i.e. the ductus arteriosus and foramen ovale. In *ex-utero* life, the two circulations are referred to as pulmonary and systemic; however, in the fetus this distinction is somewhat euphemistic, and it may be more accurate to discuss right and left circulations, a concept highlighted by Kiserud *et al.*[1]. Although studies disagree on the exact figure, there is a broad consensus that the fetal heart (in both the human and lamb model) exhibits right-sided dominance, with the majority (52–65%)[2–5] of cardiac output (CO) going through the right ventricle (RV). Of the right ventricular output the majority (75[6]–90%)[4–6] is shunted through the ductus arteriosus to the systemic circulation. Thus, it is reasonable to say that in the fetus the RV is a systemic ventricle.

Extensive investigations in developmental anatomy show that the myocardial architecture is organized as myocardial muscle fibers running in geodesic curves around toroid (doughnut-shaped) nested layers. In addition, fibers penetrate from the epicardial to endocardial layers at oblique angles to the surface geodesics. The right and left ventricles differ in the arrangement of their respective nested tori; while the left ventricle (LV) follows a more regular arrangement, the RV torus is stretched and bent to bring the pulmonary orifice forward and left of the aortic orifice. The interface of the right and left tori creates the muscular septum. The entire heart can be envisioned as 'a nested set of warped pretzels'[7] and the seminal paper by Jouk *et al.*[7] provides a detailed description.

Cardiac form develops to serve function[8]. The heart begins as a primitive tube, and the first contractions are seen at approximately 22 days in the human[9]. Next, the tube transitions to a looped heart. Soon afterward morphological differentiation of myocardium begins and chambers are formed. Finally, these stages are completed with the process of septation[8]. The geometry of the cardiac ventricles develops through the course of gestation; the myocardium undergoes a process of progressive compaction as coronary circulation develops and tissue can no longer be supplied by diffusion alone. As this ventricular architecture develops, so does the electrical excitation sequence. Activation follows blood

Correspondence to: Prof. S. Yagel, Department of Obstetrics and Gynecology, Hadassah-Hebrew University Medical Centers, Mt. Scopus, PO Box 24035, Mt. Scopus, Jerusalem, Israel 91240 (e-mail: simcha.yagel@gmail.com)

Accepted: 12 May 2011

flow, proceeding toward the outflow portion of the ventricle. As the trabeculae develop, they are activated first. Activation spreads from this interior tissue outward. In the mature trabeculated heart, activation proceeds apex-to-base[10].

The right and left sides of the heart are in no way mirror images of each other. The atria are most accurately differentiated by the extensive distribution of the pectinate muscles in the right atrium, as opposed to their relative absence in the left atrium[11]; however, the constraints of ultrasound resolution mean that the atria are usually classified as right or left morphology, based on the pulmonary and systemic venous connections. The RV is trabeculated; in particular the 'moderator band', a prominently thickened trabeculation, is a sonographic landmark that identifies the RV. The RV is also shaped more like a banana, with the pulmonary and tricuspid valves at each end. The LV is shaped more conically, like a 'ballerina's foot', and is lined with much finer trabeculations, making it appear smooth-walled on ultrasonography[12]. The ventricles are also differentiated by their respective atrioventricular valves: the RV has the three-leaflet tricuspid valve, as opposed to the two-leaflet mitral valve of the LV, although the three leaflets may not be clearly distinguishable during early fetal echocardiography. Also, the septal leaflet of the tricuspid valve joins the interventricular septum more apically than does the mitral valve[11,13].

Despite these anatomical differences, Johnson *et al.*[14] examined intracavitary pressures in 33 second- and third-trimester fetuses undergoing clinically indicated invasive obstetric procedures. The investigators found that the resulting waveforms were similar to those obtained in postnatal life. Both the LV and RV waveforms showed a small atrial component and rapid increase during systole, followed by a rapid decrease in diastole. Systolic and diastolic pressures increased linearly during gestation. There was no significant difference between left and right intraventricular pressures. The mean systolic and diastolic pressures measured approximately 20 mmHg and 5 mmHg at 20 weeks' gestation, respectively. Mean atrial pressure was approximately 3.4 mmHg in the left atrium and 3.6 mmHg in the right. No significant change was noted in intra-atrial pressure over the course of gestation. The authors concluded that changes in ventricular pressure mirror those seen in studies performed in fetal lambs and premature newborns of similar post-conceptional age at measurement. Such changes may correspond to those observed as resulting from the maturation of myocardial contractility in animal models[14].

The orientation of the heart in the fetus differs from that in *ex-utero* life. The apex of the heart is displaced cranially by the relatively large liver, at least through the second trimester. This means that the long axis of the LV is more horizontal in the fetus than in the neonate[15]. It has also been shown that the geometry of the heart and great vessels changes during gestation. The angles between the ductal arch and fetal thoracic aorta, the ductal arch and aortic arch, and the left outflow tract and main pulmonary artery all change throughout gestation and this may have ramifications for the geometrical assumptions used in volume calculations[16].

The fetal heart also reacts to damage differently from the adult heart, responding with myocyte proliferation in addition to hypertrophy[17–19]. Perhaps, for these reasons, deterioration in clinical measure of cardiac function may often be the first sign of fetal pathology[20]. Therefore, the development of sensitive methods of quantifying fetal cardiac function is of extreme importance, with a particular emphasis on the RV, as this is effectively the systemic ventricle of the fetus. With the incidence of congenital heart disease now seemingly higher than was previously thought, in particular in the neonatal intensive care unit population[21], the importance of tracking function along a time axis becomes critical for the timing of fetal interventions and other management decisions.

CARDIAC FUNCTION: BASIC PRINCIPLES

Although a detailed survey of all components of normal cardiac pump function is beyond the scope of this review, it may be timely to delineate briefly the main features. The two pumps, left and right, are each made up of an atrium which receives venous blood and a ventricle which ejects blood into an arterial system. Once the pressure in the ventricle has fallen beneath the pressure in the atrium, the atrioventricular valve opens and blood enters the ventricle, at first passively and later actively, because of atrial depolarization and contraction (the so-called 'atrial kick'). The terms 'active' and 'passive' of course refer to the macroscopic appearance, although both processes are active at the molecular level.

The atrial contribution to CO becomes more significant as heart rate increases, owing to the shortening of the passive ventricular filling time that occurs as heart rate rises. The atrial kick is one mechanism to ensure efficient ventricular filling across a spectrum of heart rates. Similarly, the sympathetic nervous system, while responsible for the positive chronotropic effect, also causes a decrease in the action potential duration, as well as an increase in the rate of cardiac relaxation, thereby reducing the loss of passive ventricular filling time at higher heart rates. As the ventricle depolarizes and contracts, pressure rises steeply within the ventricle, causing the atrioventricular (AV) valve to close. Then follows the period of isovolumetric contraction within the ventricle, leading to an increase in pressure, until the pressure in the ventricle exceeds that in the aorta or pulmonary artery, causing the semilunar valve to open and blood to be ejected forcefully into the arterial circulation. Eventually the ventricular pressure recedes, as the force of contraction decreases. Once ventricular pressure falls beneath arterial pressure, the semilunar valve closes. The time interval between the semilunar valve closing and the AV valve opening is known as the isovolumetric relaxation phase. The atrium fills continuously throughout ventricular systole, causing

a gradual increase in atrial pressure until this exceeds ventricular pressure, at which point the AV valve opens and the cycle begins again. Although there is some debate in the literature, for the purposes of this article, systole comprises isovolumetric contraction and ventricular ejection, while diastole comprises isovolumetric relaxation and ventricular filling[22].

DETERMINANTS OF STROKE VOLUME: PRELOAD, AFTERLOAD AND CONTRACTILITY

Stroke volume, the amount of blood ejected by the heart in a single beat, is principally determined by three factors: preload, afterload and contractility. The pressure within the ventricle at the end of diastole is referred to as the ventricular preload, as this is a major determinant of the ventricular volume and therefore of cardiac muscle fiber length. Starling's law of the heart states that, in the non-failing heart, the increased length of the muscle fibers results in increased energy of contraction. In other words, increased end-diastolic volume causes increased stroke volume. Afterload refers to the pressure against which the cardiac muscle fibers are shortening, and in fact is the limiting factor that determines the extent to which they are able to shorten. Thus, increased afterload results in reduced cardiac muscle shortening and, therefore, reduced stroke volume. Systemic blood pressure is usually taken as a surrogate marker of afterload. Finally, the contractility (ability to shorten) of the cardiac muscle itself is controlled by the sympathetic nervous system. Noradrenaline release causes increased contractility of the fibers, for any given preload, causing increased stroke volume.

Over the years many parameters have been proposed in an attempt to quantitatively evaluate cardiac function. Most were first developed for adult heart evaluation and were adapted to the fetus. Some are based on Doppler flow mapping, others on heart biometry or on timing of cardiac cycle events, or a combination of these three. They include stroke volume (velocity time integral × valve area), CO (stroke volume × heart rate) and ejection fraction (EF) (stroke volume ÷ end-diastolic volume). Others are the shortening fraction ((end-diastolic ventricular diameter − end-systolic ventricular diameter) ÷ end-diastolic ventricular diameter); myocardial ejection force ((1.055 × valve area × velocity time integral of acceleration) × peak systolic velocity ÷ acceleration time); and myocardial performance index (MPI) ((isovolumetric contraction time + isovolumetric relaxation time) ÷ ejection time). These formulae are summarized in Table 1. As in evaluation of pediatric and adult heart function, any cardiac biometry, and functional measures based on heart or vessel dimensions, will necessarily correlate with body size.

Stroke volume (SV) is a calculation of blood flow out of the heart at systole. However, measurement of the ventricular volume is cumbersome. In the left heart, therefore, SV is based on measurement of diameter of the aorta at the valve annulus to determine valve area, multiplied by flow across the annulus, represented by the time velocity integral. Right SV is calculated from the diameter of the pulmonary artery. Any inaccuracy in diameter measurement will introduce considerable error into the calculation, since this number is squared to obtain the valve area. Thus, SV is necessarily an indirect measure of the blood volume exiting the ventricle. CO is SV multiplied by fetal heart rate. Mielke *et al.*[3] examined SV and CO in 222 fetuses from 13 weeks' gestation to term. They showed that SV increases exponentially as gestation progresses. Median biventricular CO ranged from 40 mL/min at 15 weeks up to 1470 mL/min at 40 weeks; the median CO per fetal weight was 425 mL × min^{-1} × kg^{-1} and the median right/left CO ratio was approximately 1.4, remaining stable throughout gestation and underscoring right heart dominance in the fetus[3]. Three-/four-dimensional ultrasound (3DUS/4DUS) techniques to evaluate fetal heart function often are used to determine fetal ventricular volume, to enable direct quantification of fetal SV and CO and this is discussed below.

Table 1 Formulae for fetal cardiac functional evaluation

Index	*Formula*
Stroke volume (SV)	velocity time integral × valve area*
Cardiac output (CO)	SV × heart rate
Ejection fraction (EF)	SV ÷ end-diastolic volume
Shortening fraction (SF)	(end-diastolic VD − end-systolic VD) ÷ end-diastolic VD
Myocardial ejection force	(1.055 × valve area × velocity time integral of acceleration) × peak systolic velocity ÷ acceleration time
Myocardial performance index (MPI)	(ICT + IRT) ÷ ET

*Aortic or pulmonary (see text for details). ET, ejection time; ICT, isovolumetric contraction time; IRT, isovolumetric relaxation time; VD, ventricular diameter.

M-MODE

M-mode echocardiography is the study of two-dimensional motion of all structures along an ultrasound beam over time. It was first described for assessment of cardiac function in 1971 in adults[23], and normal values in the fetus were published in 1982[24]. It allows for calculation of the shortening fraction, the change in ventricular diameter between end diastole and end systole as a ratio of the end-diastolic diameter, which is a long-standing surrogate for function[25]. Disadvantages include the difficulty in obtaining the correct view in a fetus, a line perpendicular to the interventricular septum at the level of the AV valve leaflets[26], depending on fetal lie (Figure 1). However, it is used as a component of other techniques, most notably annular displacement (see below).

Annular excursion/displacement uses M-mode echocardiography to measure the maximal excursion of the junction between the tricuspid annulus and the RV free wall, from end diastole to end systole. It is a measure of

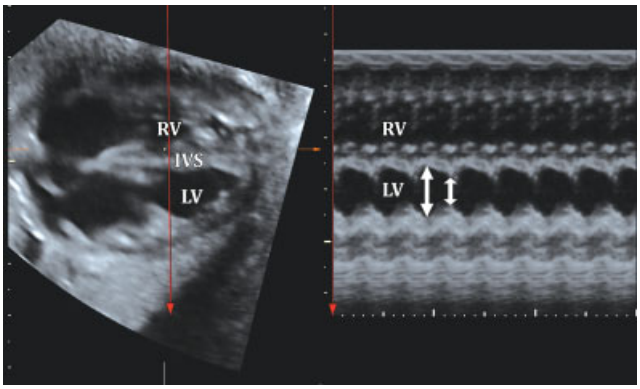

Figure 1 M-mode measurement of end systole and end diastole performed in a spatiotemporal image correlation volume. After acquisition, the volume is adjusted to show the four-chamber view. The M-mode cursor is placed perpendicular to the interventricular septum (IVS). Arrows mark end diastole and end systole. LV, left ventricle; RV, right ventricle.

RV function that has been shown in adults to have prognostic significance independent of LV function[27]. In the fetus, M-mode evaluation of annular displacement of both the mitral and tricuspid valves is a feasible technique[28], and amplitude has been shown to increase with gestational age[29]. Annular displacement techniques essentially use M-mode to measure long-axis function as opposed to short-axis function, which is more commonly associated with M-mode measurements[29]. This technique is most suited to RV examination because of the longitudinal orientation of the deep RV muscle fibers, as opposed to the mainly circumferential arrangement of LV muscle fibers[29,30]. This technique has the advantage of utilizing M-mode technology that is readily available with modern ultrasound machines. However, it has not yet been evaluated fully or compared with other methods of assessing function in the fetus.

EARLY/ATRIAL (E/A) RATIO (ATRIOVENTRICULAR FLOW)

The E/A ratio refers to the ratio of the two peaks in flow velocity observed over the atrioventricular valves during diastole. The E-wave is the early, passive diastolic filling, which is dependent on ventricular wall relaxation. The A-wave is the active diastolic filling known as the 'atrial kick'[31]. It is measured using pulsed-wave (PW) Doppler echocardiography, with the cursor set on or just below the AV valve (usually the mitral) in a four-chamber view. *Ex utero*, under normal conditions, the E-wave is greater than the A-wave. In the healthy fetus, the A-wave is usually greater, although as gestation progresses, the E/A ratio increases, approaching the *ex utero* values (Figure 2). It is generally agreed that increase in the E/A ratio is due to increasing E-wave velocity, while the A-wave remains fairly constant throughout gestation, although there is some dispute as to whether the velocity increases linearly throughout gestation[32,33] or only in the last trimester[34]. The increase in E-wave is thought to result from improved ventricular relaxation[35]. Since ventricular relaxation

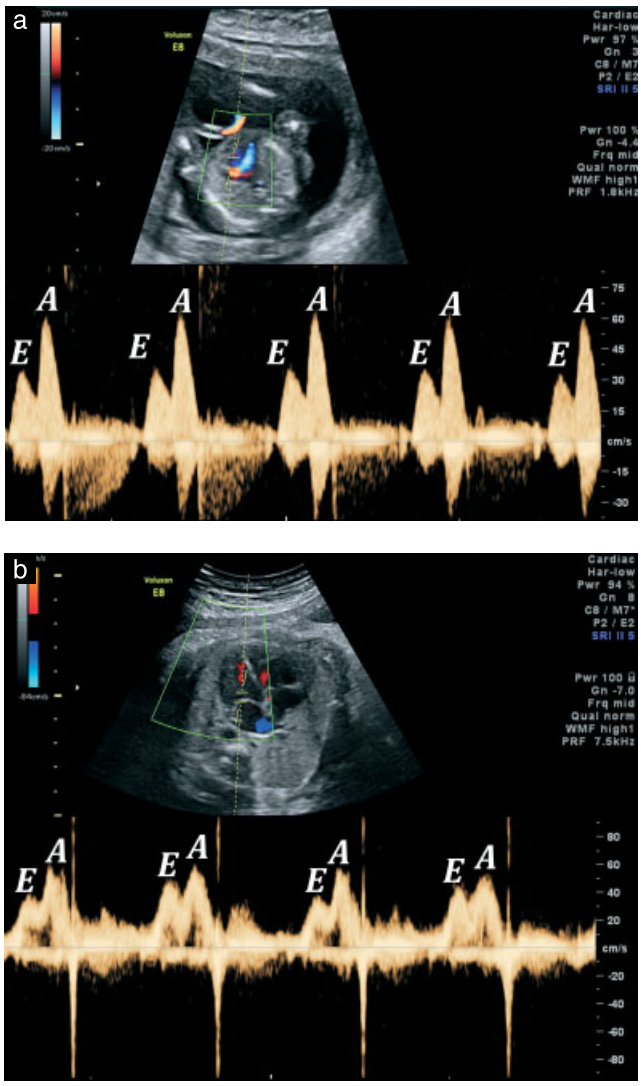

Figure 2 Spectral Doppler trace of the E/A-wave in a 15-week fetus (a) and a 35-week fetus (b), showing the progressive increase in ventricular compliance during pregnancy.

allows for coronary blood flow[36], it would be expected that this too is increased throughout gestation; however, experimental evidence so far has shown that coronary blood flow remains constant throughout gestation[37].

In adult life, reduction in the E/A ratio is a sign of diastolic dysfunction, associated with poor prognosis in patients with congestive heart failure[38]. In the fetus, a reduction in both mitral and tricuspid E/A ratio has been reported in recipient twins in twin–to–twin transfusion syndrome (TTTS), along with other markers of diastolic dysfunction[39]. However, other studies have shown an increase in E/A ratio in situations of cardiac compromise, including intrauterine growth restriction (IUGR) and hydrops due to congenital cystic adenomatoid malformation[40,41].

It has been shown that the E/A ratio shows poor correlation with isovolumetric relaxation time[42,43] as well as venous flow patterns[44]. However, the lack of an objective reference standard for measuring fetal cardiac function makes it difficult to compare one test with

another, as each has its own methodological limitations. Qualitatively, monophasic AV flow patterns, with complete absence of the normal biphasic E/A morphology, indicates severe CO pathologies, such as aortic stenosis[45] and TTTS[46], and is a poor prognostic indicator in cases of IUGR[47]. This pattern should not be mistaken for fusion of E- and A-waves that occurs physiologically at high heart rates[48]. The E/A ratio has the advantage of allowing measurement of both sides of the heart independently, although it is a marker of diastolic function (Figure 2).

MYOCARDIAL PERFORMANCE INDEX

The MPI or Tei index is the sum of the isovolumetric contraction and relaxation times, divided by the ejection time. It was first reported as a measure of global cardiac function in 1995[49]. The index comprises both systolic and diastolic components, and can be used to analyze each ventricle independently. It has the advantage of not requiring a detailed anatomical survey in order to analyze function[50]. It is obtained by echocardiographic evaluation of the flow patterns through the AV valves and outflow tracts. The ejection time is measured as the duration of flow through the outflow tract, e.g. aortic valve. The isovolumetric contraction time is the interval between cessation of AV valve flow and the onset of outflow tract flow. The isovolumetric relaxation time is the interval between cessation of outflow tract flow and the onset of AV valve flow. The flow patterns are usually obtained with PW Doppler, but can also be obtained using M-mode and tissue Doppler imaging (TDI). As it utilizes only time intervals, it is independent of heart rate and ventricular structure [20,51]. Its use in fetal echocardiography was first reported in 1999, when Tsutsumi *et al.* showed that the Tei index can be used in fetuses, and that there is a decrease in the Tei index of both ventricles during gestation, with a transient increase immediately after birth[52]. Subsequently, it was suggested that the use of 'clicks' could help standardize the boundaries of the isovolumetric waveform durations. These clicks represent the Doppler echoes from the closure of the mitral and aortic valves, and provide a convenient objective standard for defining the boundaries of valvular flow (Figure 3). Thus, Hernandez-Andrade *et al.* demonstrated reduced inter- and intrauser variability with the incorporation of clicks into the calculation of the Tei index[53]. Using this 'modified MPI', they then demonstrated, contrary to Tsutsumi *et al.*, that there is a slight increase overall in the LV Tei index from gestational week 19 onwards, with isovolumetric relaxation time increasing, ET decreasing and isovolumetric contraction time remaining constant[54]. These results are also contrary to those of van Splunder and Wladimiroff in 1996, who essentially measured the same variables, although not referring to the Tei index, and found that left ventricular ET and isovolumetric relaxation time both decrease with gestational age[55], with no significant change in isovolumetric contraction time, admittedly with a much smaller number of subjects than were included in the study by Hernandez-Andrade *et al.* (52 vs. 557, respectively). Van Mieghem *et al.* showed the Tei index to correlate well with the EF in the fetus, with the advantage of less inter- and intraexaminer variability, thus validating the use of the Tei index in fetal echocardiography. Interestingly, they found no significant correlation between the E/A ratio and the Tei index, as well as no change in the Tei index with gestational age[56].

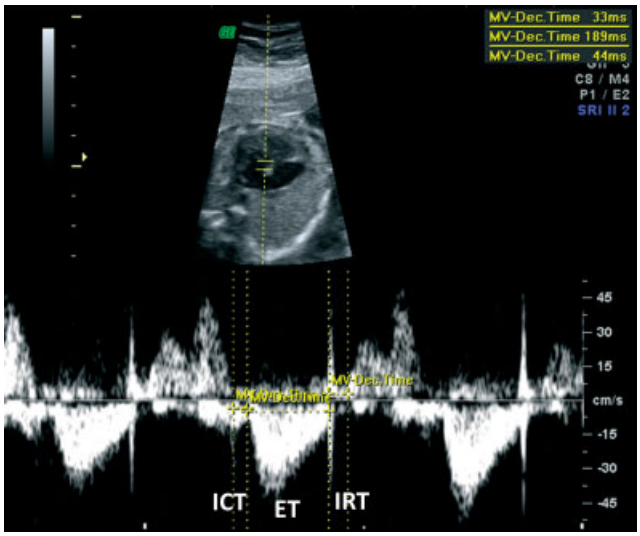

Figure 3 Myocardial performance index (MPI) measured by valve clicks in the Doppler trace. MPI = (ICT + IRT) ÷ ET. Caliper placement is indicated by dotted lines. ET, ventricular ejection time; ICT, isovolumetric contraction time; IRT, isovolumetric relaxation time.

The Tei index as measured in the fetus has advantages over its application in the adult heart. Friedman *et al.* showed that in the fetus one can measure the mitral and aortic valve flows simultaneously[50], thereby removing the inaccuracy involved in measuring the time intervals across different heart beats. However, the right-sided valves, due to their different anatomical configuration, cannot be captured simultaneously. Perhaps for this reason the right side is less frequently included in MPI research. However, as has been mentioned, in adult cardiology, where the MPI was first utilized, neither side can be assessed simultaneously using flow Doppler techniques[51]. One technique to minimize the inaccuracy induced by measuring time intervals across different heart beats is taking the average of the MPI as obtained across several heart beats[52]. The application of tissue Doppler techniques to the MPI has been shown to enable simultaneous appraisal of inflow and outflow, both in the fetus[57] and adult[58]. However, there is not yet a consensus that TDI and pulsed-wave Doppler evaluation of MPI give the same results[59].

The MPI has been widely studied in a number of fetal pathologies. In TTTS the MPI has been shown to be pathological in the recipient twin, due to a prolongation of the isovolumetric relaxation time, implying diastolic dysfunction[60]. This is in contrast to results in fetuses suspected of suffering from fetal inflammatory response syndrome due to infection secondary to premature rupture of membranes. In the latter case the MPI is also increased, implying reduced function, but the increase is

due to a shortening of the ejection time, the denominator of the Tei index formula[61]. In fetuses with homozygous α-thalassemia (Hb Bart's fetal edema), a cause of fetal demise with progressive cardiac dysfunction, the MPI is elevated as early as week 20, long before ventricular and atrial enlargement occur[57]. The Tei index has also been shown to be elevated in hydrops fetalis, as well as in large-for-gestational age fetuses of diabetic mothers[62], although the clinical significance of the latter finding is not clear. Crispi *et al.* demonstrated an increase in MPI with increasing severity of IUGR, with both diastolic and systolic components affected, as well as an association between increased MPI and fetal death[41].

Thus, it has been shown that a raised MPI value is a sensitive, albeit non-specific, marker of fetal cardiac dysfunction. However, the Tei index has been shown to have some limitations. Firstly, competence in the technique itself seems to be somewhat challenging to acquire, as demonstrated by Cruz-Martinez *et al.*[63]. It takes on average 65 exams before the inexperienced practitioner can achieve competence in this skill. This limits the applicability of the Tei index to high-volume referral centers, in which practitioners will be able to develop and maintain competence.

There have also been certain clinical contexts in which the Tei index has been shown to be unreliable. In a study of adults with aortic stenosis and reduced LV function, Sud and Massel showed that the Tei index remains unchanged in severe aortic stenosis despite worsening EF, and that the index paradoxically decreases as the aortic stenosis gets more severe in patients with reduced EF[64]. Using ROC curves, the index was shown to be unable to identify accurately patients with reduced LV function in the presence of severe aortic stenosis, as well as patients with severe aortic stenosis in the presence of reduced LV function. Another concern has been raised regarding the use of the Tei index in cases of pulmonary hypertension. The index has been reported to correlate with pulmonary hypertension in both adults[65] and children[66]. Translating these concepts to fetal medicine, the paradigm of increased fetal RV afterload is ductal constriction. Mori *et al.* found the Tei index to be increased in cases of ductal constriction, and suggest that it can be used as a sensitive marker of RV dysfunction in this condition[48]. However, concerns have been raised as to the legitimacy of using time intervals to assess function in pulmonary hypertension, since time intervals are themselves related to RV afterload. Thus, given an abnormal Tei index in cases of elevated pulmonary artery pressure or ductal constriction, it may be that the index is caused by the elevated afterload, and not directly by RV myocardial dysfunction[67]. Similarly, Cheung *et al.* found that the Tei index was not sensitive to dobutamine infusion in anesthetized pigs, but was sensitive to changes in preload and afterload[68]. This is in contrast to the results published by Eidem *et al.* which showed no effect of loading conditions on the Tei index in adults and children with congenital heart disease before and after surgery[69]. As such, it has been suggested that the Tei index be viewed as a 'sedimentation rate of the heart', an indication of pathology, with perhaps limited ability to reflect causality[69]. However, the reproducibility[56] of the MPI, as well as its sensitivity, make it, in the opinion of the authors, an important tool in fetal echocardiography, including the timing of interventions.

THREE- AND FOUR-DIMENSIONAL ULTRASOUND

3DUS/4DUS technologies have been used over the last decade to evaluate fetal cardiac function, chiefly with the aid of spatiotemporal image correlation (STIC)[70]. STIC is based on a sweep of the fetal heart comprising the five transverse planes approach[71], and delivers a volume dataset containing a complete reconstructed cardiac cycle, made up of approximately 1500 images. The operator can navigate both spatially and temporally within the saved dataset. Thus, for example, the four-chamber view at end diastole and end systole can be identified by valve movement, and from these starting points either manual or semi-automated volume measurement of the cardiac ventricles is possible. The studies of 3DUS/4DUS applied to fetal heart function evaluation are based primarily on cardiac ventricular volumetry and cardiac valve clicks. The goal of all these methods has been extrapolation of fetal stroke volume, EF and CO from the resulting ventricular volumes[72–76] (Figures 4 and 5).

Manual volumetry based on STIC volumes obtained by segmentation was studied by Uittenbogaard and colleagues[75]. The ventricles are manually traced in multiple serial slices 1 mm apart; these were obtained by scrolling through the saved volume in multiplanar reconstruction, and Simpson's rule was applied[75]. Alternatively, semiautomated segmentation involves specialized

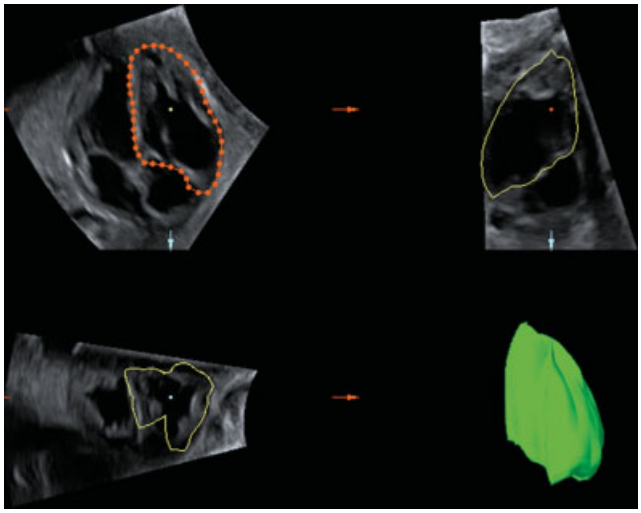

Figure 4 Ventricular volume measured with Virtual Organ Computer-aided AnaLysis (VOCAL). The application is opened and the operator traces the ventricular borders at a preset number of planes as the system rotates around a fixed axis. The system then computes the contour of the measured organ, in this case the cardiac ventricle (lower right frame).

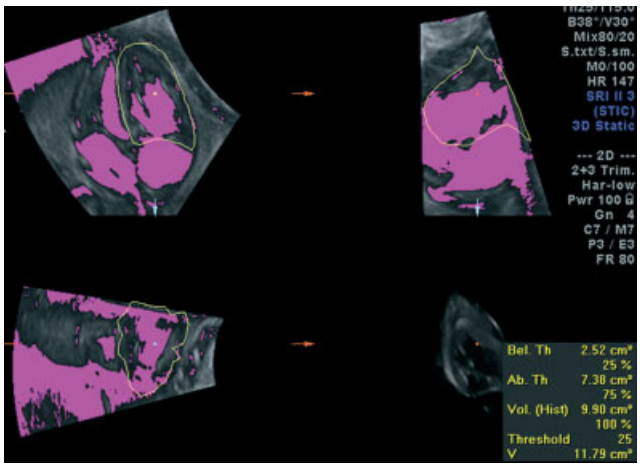

Figure 5 Ventricular volume calculated using Virtual Organ Computer-aided AnaLysis (VOCAL) combined with inversion mode (IM). The addition of IM helps to isolate the fluid-filled intracardiac volume from the papillary muscles and the ventricular walls and septum.

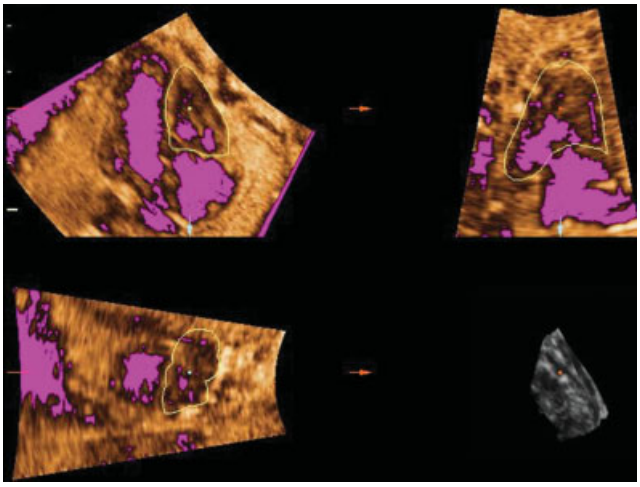

Figure 6 A case of pulmonary stenosis evaluated with Virtual Organ Computer-aided AnaLysis (VOCAL) and inversion mode. The right ventricular volume, normally greater than that of the left in the fetus, is markedly decreased.

algorithms applied to the STIC volume[72–74,76–78]. Virtual Organ Computer-aided AnaLysis (VOCAL), which measures the volume of a defined area by reconstructing planes around a fixed central axis, is initiated and the volume of the organ of interest is determined (Figure 4). VOCAL may be combined with inversion mode (IM)[73], which isolates fluid-filled areas (black) from tissue (gray) and inverts their representation (Figure 5).

We found that ventricular volumetry successfully differentiated between normal and anomalous hearts. For example, Figure 6 shows a case of pulmonary stenosis at 32 weeks' gestation, with RV volume significantly decreased from the mean (RV end-diastolic volume measured 0.7 (mean, 2.71) cm^3 and RV end-systolic volume measured 0.37 (mean, 1.34) cm^3, both below the 5% CI for the mean for gestational age)[73]. We extended the combination of VOCAL and IM used for ventricular volumetry[73] to calculate ventricular mass. Applying the algorithm we were able to deduct the intraventricular volume from the total ventricular volume automatically, the remainder being the volume of the myocardium. This was multiplied by estimated fetal cardiac density (1.050 g/cm^3)[79] to obtain the mass[80]. While these methodologies show promise for clinical application, they are still in their infancy, requiring a long learning curve and considerable operator expertise. If a viable automated program for ventricular volumetry and its related measures are introduced, making the techniques less operator-dependent, they may provide additional alternatives for fetal cardiac functional evaluation.

TISSUE DOPPLER IMAGING, STRAIN AND STRAIN RATE

TDI refers to the application of Doppler principles to the measurement of the velocity of the myocardium rather than that of intracardiac blood flow (Figures 7 and 8). Since the cardiac apex remains relatively stationary throughout the cardiac cycle, analysis of the motion of the mitral valve annulus relative to the apex gives a good approximation of the longitudinal contractility of the ventricle[81]. Pulsed-wave tissue Doppler examination of the mitral annulus longitudinal motion gives three waveforms: S′, the velocity of the systolic downwards motion of the annulus towards the apex – a positive deflection waveform; E′, the velocity of the early diastolic movement away from the apex – a negative deflection waveform; A′, the velocity of the movement of the annulus associated with atrial contraction – a negative deflection waveform. The prime (′) notation is used to differentiate from the E and A waveforms of mitral Doppler inflow velocities; however, some researchers prefer the nomenclature Sa, Ea and Aa, and others use Sm, Em and Am. TDI measures the peak velocity of the myocardial segment being interrogated, unlike color TDI (see below) which measures the mean velocity[82].

Broadly speaking, S′ corresponds with LV systolic function, and has been shown to correlate with EF as measured by 3DUS[83]. Changes in the S′ waveform have been demonstrated as soon as 15 seconds after the onset of ischemia in experimental animal models[84]. E′ corresponds with diastolic function, and has been shown to be less preload-dependent than the E/A profile[85]. It can be combined with the mitral inflow, as the E/E′ ratio, which is an even more sensitive measure of diastolic dysfunction[86]. The A′ waveform has been shown to be more sensitive than the AV valve inflow profile in detecting atrial mechanical dysfunction[87].

TDI of fetal myocardium was first reported as a feasible technique in 1999[88]. Since then there have been conflicting reports as to its usefulness in the assessment of fetal heart function. RV TDI alone could not differentiate between fetuses with and without heart failure, although incorporating TDI into other techniques – the E/E′ ratio, and use of TDI to measure the Tei index, did differentiate

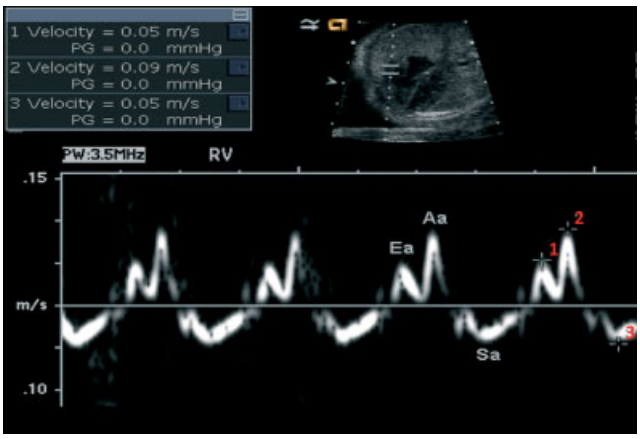

Figure 7 Axial pulsed-wave tissue Doppler echocardiography of the right ventricle showing velocities in systole and diastole. Aa, movement of the myocardium associated with atrial contraction; Ea, velocity of early diastolic movement away from the apex; Sa, systolic downwards motion of the myocardium towards the apex. (Image courtesy of Prof. Jack Rychik).

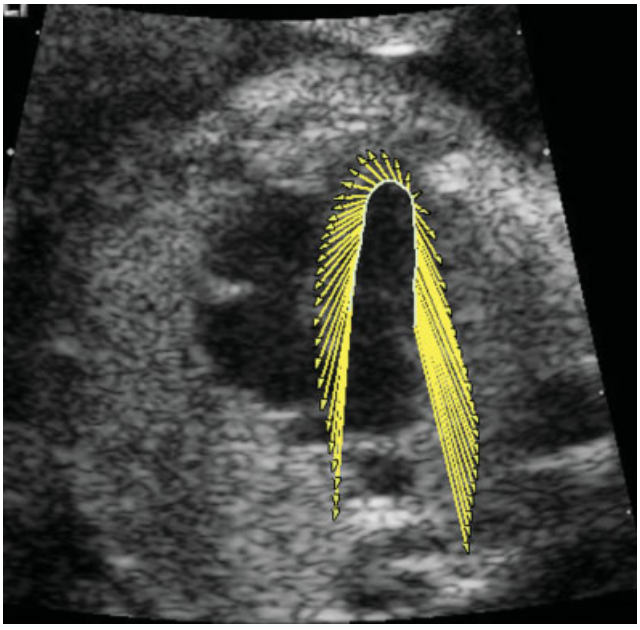

Figure 8 Left ventricular velocity vector image. On this still frame of the left ventricle, the length of each arrow represents the velocity amplitude, while the direction reflects motion of the myocardium. (Image courtesy of Prof. J. Rychik).

between the groups[89]. A more recent study showed a significantly reduced LV-S′, as well as an increased E/E′ ratio and RV-S′/LV-S′ in a group of fetuses with hydrops fetalis, as compared to normal controls[90]. Similarly, it has been reported recently that TDI is more sensitive than 'conventional' AV flow and MPI measurements in detecting systolic and diastolic dysfunction in IUGR fetuses[91]. It is unclear if there is any clinical significance in the increased sensitivity of TDI in IUGR, e.g. if it marks out a subgroup of fetuses that have a poorer prognosis. Alternatively, TDI may be just a more sensitive technique, picking out the lower end of 'normal', with no functional or clinical significance.

The main disadvantages of PW-TDI are that it can provide information about only one area of the myocardium at any one time[48] as well as being very angle-dependent, i.e. only those areas of the myocardium that are parallel to the angle of insonation can be analyzed[92]. The application of color Doppler to TDI enables the assessment of strain rate (change in length per unit time), and, by mathematical derivation, myocardial strain (change in length) itself[93]. These modalities have the advantage of directly measuring myocardial segments, as opposed to chamber-dimension changes, and thus should reflect myocardial contractility more accurately[20,29,40]. However, they suffer from the same drawbacks as PW-TDI, namely angle dependency and assessment of individual segments rather than global function.

SPECKLE TRACKING

A relatively recent approach to studying myocardial motion as a surrogate for cardiac function is the use of speckle-tracking techniques. These use 2D B-mode echocardiography, and are based on identifying 'speckles'. Speckles are natural acoustic markers, spread randomly throughout the myocardium, which are generated by stable interference and backscatter of the ultrasound signal[80,94]. These speckles are identified, and their positions are noted in subsequent frames in a cineloop. With the frame-rate a known quantity, the velocity vectors for each speckle can be calculated and, thereby, the strain and strain rate can be evaluated segmentally as well as for the whole chamber. Speckle tracking is usually coupled with an automated border recognition program, so that speckle tracking occurs within the context of the ventricle under investigation. This combination of software allows for estimation of the EF as well as direct measurement of strain and strain rate. Speckle tracking essentially measures myocardial deformation (change of shape) as opposed to the point changes in velocities measured by TDI[95].

Speckle tracking is limited, however, to speckles which remain within the imaging plane throughout the cardiac cycle. Speckles which pass through the plane of insonation cannot be tracked, at least not by the majority of current systems[96]. However, a recent study by Matsui *et al.* has shown that speckle tracking, which requires offline processing with dedicated software, is no better than is M-mode for measuring annular displacement techniques, which is readily performed on any modern ultrasound machine[97].

Perk *et al.* compared EF estimation by speckle tracking, by applying the standard 'Simpson's rule' (measuring end-diastolic and end-systolic volumes manually) and by visual examination by an experienced echocardiographer. They found strong correlation among all three methods[94]. This too begs the question as to the usefulness of a technique which is equivalent to, but less accessible than, older technology. The authors do not provide data about the total time required to perform and process the speckle-tracking studies as opposed to the M-mode assessment of

EF. Matsui *et al.*[97] also noted that, conceptually, there is a problem in applying color Doppler techniques to the fetus, where the ratio of pixel to myocardial volume is much higher than in the adult. This is presumably true of speckle-tracking techniques as well. Also, the technique is dependent on frame-rate of the ultrasound machine, and it has been suggested that the frame-rates in most current machines are too low to allow accurate speckle tracking in the fetus. This is in part owing to the lack of ECG gating in fetal echocardiography. The authors demonstrated that interposing a metronome to artificially generate simulated ECG spikes, thereby enabling the images to be stored at a higher frame rate, caused an increase in successful speckle-tracking acquisition[97]. As has been mentioned, speckle tracking, as well as Doppler-derived measures of strain, have the advantage of providing both segmental and global functional information concerning both the left and right heart in systole. Speckle tracking has not yet been studied sufficiently for use in evaluation of diastolic function, and the use of TDI for diastolic evaluation is limited to certain subgroups in adults[98].

MAGNETIC RESONANCE IMAGING

Since the advent of magnetic resonance imaging (MRI) in the 1980 s as a research, and subsequently clinical, tool it rapidly became an important adjunct for assessment of cardiac structure and function (both systolic and diastolic) *ex-utero*[99]. Fetal circulatory physiology and many congenital lesions make accurate depiction of RV structure and function critically important, and MRI is currently considered the reference standard for *ex-utero* RV assessment[100,101]. MRI, both *in utero* and *ex utero*, enables measurement and calculations of ventricular volumes and mass, as well as EF and CO/cardiac index. Unlike ultrasonographic techniques, MRI is not affected by maternal obesity or oligohydramnios[102], and image quality is not dependent on gestational age[103]. Since it does not rely on assumptions, but rather on true real-time measurements, it is useful for the examination of abnormal hearts that do not conform to the geometric models used in ultrasound techniques[104]. Other advantages include better image quality and structural detail[105]. Technical disadvantages include the expense of the technique, the relatively long duration of the examination (although this is reported to be as short as 15 minutes in some studies[101]) and the lack of availability of both the technology and expertise to perform the examination. Some centers advocate using a sedative premedication to reduce fetal movements; however, as technology improves and study times shorten, this will no longer be required[106].

Historically, fetal MRI techniques have been hampered by the lack of ECG-triggering, which is typically used in *ex-utero* cardiac MRI. However, experimental techniques have been developed in the chick embryo which could bypass this requirement[107]. Another concern is the problem of temporal resolution, due to the time required to acquire images, in the context of rapid fetal heart rate; however, there are feasibility studies showing that modern MRI sequences are able to acquire fetal cardiac MR[94,104].

VENOUS FLOW ASSESSMENT

Analysis of the flow (by PW Doppler) within venous channels contiguous with the RA (ductus venosus, inferior vena cava, hepatic veins and pulmonary veins (DV, IVC, HV and PV, respectively), excluding the umbilical vein (UV) which is non-pulsatile from the end of the first trimester[108]), gives a good approximation of the pressure gradients within the atrium itself (Figure 9). The major veins all exhibit a pulsatile flow waveform, representing changes in pressure during the cardiac cycle, with forward venous flow facilitated by low atrial pressures. Thus, at those points within the cycle where atrial pressure is lowest, forward venous flow will be maximal, and where atrial pressure is highest, venous flow will be minimal or even reversed. The normal waveform is the S-wave (maximal forward flow corresponds to ventricular systole, with rapid descent of the closed AV valves causing a drop in atrial pressure), v-descent (ventricular relaxation with rising AV valves, causing a temporary increase in atrial pressure), D-wave (early ventricular diastole, with blood rushing forward into the ventricles, causing a drop in atrial pressure) and a-wave (atrial systole, or atrial kick with pressure in atrium rising steeply)[109].

The most significant change in venous Doppler with cardiac dysfunction is reversal or absence of the a-wave, which portends serious consequences in cardiac pump function, with a subsequent daily risk of worsening fetal wellbeing and intrauterine death[109] (Figure 10). Reversal of the a-wave in the DV in fetuses aged 11–14 weeks has been shown to be associated with a 25% chance of congenital heart defects[110], and in high-risk fetuses aged 26–34 weeks, absent or reversed a-wave was associated with a 63% risk of fetal or neonatal death[44]. This finding is also indicative of Stage III in the Quintero staging of TTTS[111]. Another venous waveform with prognostic significance is pulsatile flow in the umbilical vein, which has been shown to correlate with the

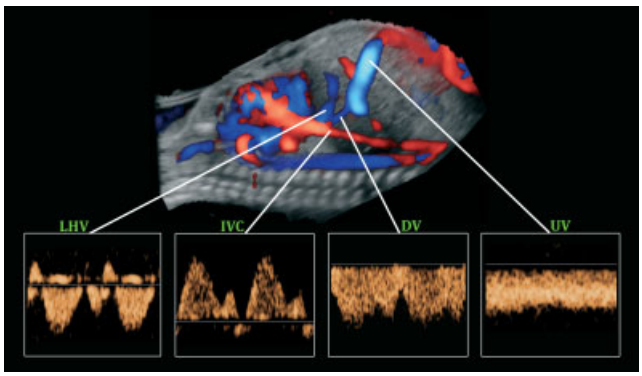

Figure 9 The fetal abdomen in sagittal plane, showing the sampling sites and normal Doppler waveforms in the left hepatic vein (LHV), inferior vena cava (IVC), ductus venosus (DV) and umbilical vein (UV). (Reproduced with permission from Yagel *et al.*[123]).

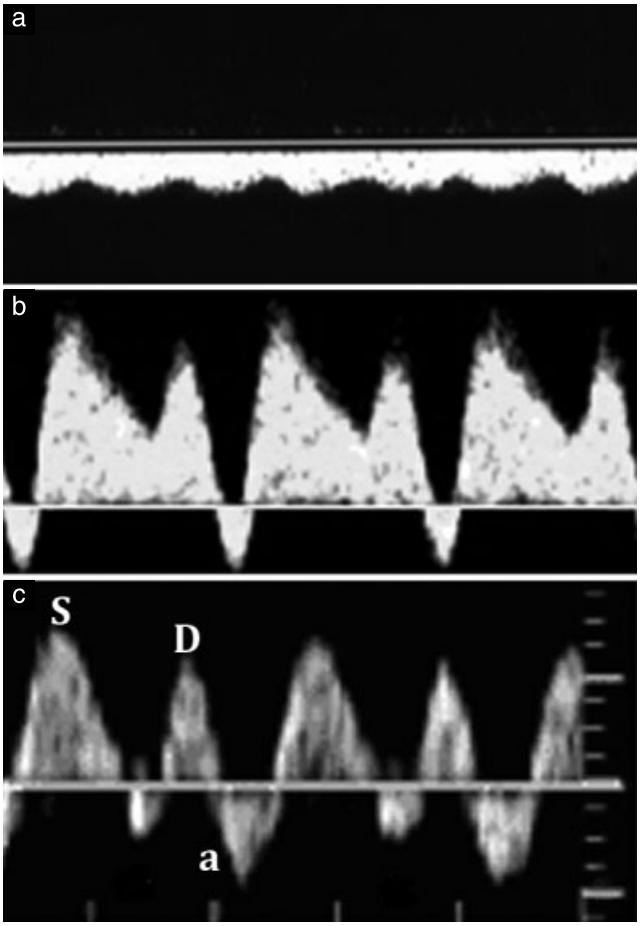

Figure 10 Abnormal Doppler waveforms in the: (a) umbilical vein (UV), (b) ductus venosus (DV) and (c) inferior vena cava (IVC). (a) An abnormal UV waveform in hemodynamically compromised fetuses is characterized by the appearance of pulsations. (b) The DV normally has forward blood flow throughout the cardiac cycle. In compromised fetuses a drop in atrial systolic forward velocities is observed. As central venous pressure increases, blood flow may be reversed during atrial systole. (c) Abnormal IVC waveforms in intrauterine growth restriction show a decrease in forward flow during the S-wave (S) and D-wave (D) and accentuation of reversed flow in the A-wave (annotated 'a'). As the condition deteriorates, the D-wave may be reversed. (Reproduced with permission from Yagel *et al.*[124]).

presence of myocardial dysfunction[112]. Although the UV is non-pulsatile under normal conditions, the presence of pulsatile flow in the UV beyond the first trimester is yet another sign of cardiac dysfunction. It is a marker of progressive placental dysfunction[113], and has been shown to correlate with elevated troponin levels in the neonate[114].

Various indices of venous flow profile have been devised. One of these, the pulsatility index for veins, is the peak systolic velocity minus the peak diastolic velocity, divided by the time-averaged maximum velocity. In fetuses with IUGR, a raised ductus venosus pulsatility index for veins (DV-PIV) is indicative of a ten-fold acceleration of deterioration[113]. In a study examining neonates with elevated levels of troponin or N-terminal pro-atrial natriuretic peptide (NT-pro-ANP), markers of myocardial damage and dysfunction, respectively, elevated PIV in the fetal DV, left hepatic vein and IVC was shown to correlate with elevated umbilical artery NT-pro-ANP in specimens drawn immediately after delivery. The PIV was also highest in the subgroup of neonates with elevated levels of both troponin and NT-pro-ANP[115]. A more recent study by the same group showed that N-terminal pro-brain natriuretic peptide (NT-pro-BNP), another marker of cardiac dysfunction, was also correlated with elevated PIV[116].

Another way of examining cardiac function, as expressed in the venous system, is by analysis of the vessel pressure waveform. Mori *et al.* have shown that one can measure the changes in vessel diameter, providing a waveform that is equivalent to the central venous pressure waveform, with 'A' and 'V' peaks, and 'X' and 'Y' troughs[117]. Elements of the morphology of the waveform, in particular shortening of the A-X-V time and reduction in the X nadir, can be indicative of fetal cardiac dysfunction[118].

The utility of fetal venous Doppler examination lies in its predictive powers. Pathological changes in the venous Doppler results in growth-restricted fetuses precede changes in the cardiotocogram and biophysical profile, in some cases by a period of weeks[119,120]. Although there remains controversy among obstetricians regarding the benefits of early vs. delayed delivery in IUGR, Doppler studies (including arterial) are reported to be the most accurate non-invasive modality for assessing placental function, and therefore provide the information on the basis of which these decisions can be taken[121].

COMMENT

The focus of ultrasound scanning is shifting from the purely descriptive towards a functional, quantitative modality[122]. This results from both technological advance in ultrasound machines as well as in the progress of dedicated examiners. The techniques described above are all designed to establish markers of fetal cardiac dysfunction, in the absence of an accepted reference standard. Essentially, they all suffer from the shortcoming that, while they may strongly imply the presence of cardiac dysfunction, they do not necessarily pinpoint the etiology or causal mechanism. These modalities are perhaps most appropriate when there is a known pathology that is being followed. Many of the modalities have been tested extensively on the LV, but less so on the right. Conversely, some, such as short-axis shortening fraction, are used for analysis of the RV, even though anatomically and geometrically they are less applicable to that ventricle.

The ideal test of fetal cardiac function should be applicable mainly to the RV which, as mentioned above, is the dominant ventricle in the fetal cardiovascular system; it should be accessible using standard ultrasound machines, without relying on offline post-processing; and it should be able to predict cardiac dysfunction before there are clinical signs of fetal distress. It would seem to the authors that simple modalities such as M-mode

annular displacement, precordial venous Doppler flow assessment and MPI are the only ones to have truly crossed the translational divide between the experimental and clinical, and that can be recommended for clinical practice.

REFERENCES

1. Kiserud T, Rasmussen S, Skulstad S. Blood flow and the degree of shunting through the ductus venosus in the human fetus. *Am J Obstet Gynecol* 2000; **182**: 147–153.
2. Sutton MS, Groves A, MacNeill A, Sharland G, Allan L. Assessment of changes in blood flow through the lungs and foramen ovale in the normal human fetus with gestational age: a prospective Doppler echocardiographic study. *Br Heart J* 1994; **71**: 232–237.
3. Mielke G, Benda N. Cardiac output and central distribution of blood flow in the human fetus. *Circulation* 2001; **103**: 1662–1668.
4. Rudolph AM. Distribution and regulation of blood flow in the fetal and neonatal lamb. *Circ Res* 1985; **57**: 811–821.
5. Rudolph AM, Heymann MA. Circulatory changes during growth in the fetal lamb. *Circ Res* 1970; **26**: 289–299.
6. Rasanen J, Wood DC, Weiner S, Ludomirski A, Huhta JC. Role of the pulmonary circulation in the distribution of human fetal cardiac output during the second half of pregnancy. *Circulation* 1996; **94**: 1068–1073.
7. Jouk PS, Usson Y, Michalowicz G, Grossi L. Three-dimensional cartography of the pattern of the myofibres in the second trimester fetal human heart. *Anat Embryol (Berl)* 2000; **202**: 103–118.
8. Sedmera D. Function and form in the developing cardiovascular system. *Cardiovasc Res*.
9. Sadler T. *Langman's Medical Embryology*. Williams & Wilkins: Baltimore, USA, 1985.
10. Sedmera D. Form follows function: developmental and physiological view on ventricular myocardial architecture. *Eur J Cardiothorac Surg* 2005; **28**: 526–528.
11. Uemura H, Ho SY, Devine WA, Kilpatrick LL, Anderson RH. Atrial appendages and venoatrial connections in hearts from patients with visceral heterotaxy. *Ann Thorac Surg* 1995; **60**: 561–569.
12. Cook AC, Yates RW, Anderson RH. Normal and abnormal fetal cardiac anatomy. *Prenat Diagn* 2004; **24**: 1032–1048.
13. Yagel S, Benachi A, Bonnet D, Dumez Y, Hochner-Celnikier D, Cohen SM, Valsky DV, Fermont L. Rendering in fetal cardiac scanning: the intracardiac septa and the coronal atrioventricular valve planes. *Ultrasound Obstet Gynecol* 2006; **28**: 266–274.
14. Johnson P, Maxwell DJ, Tynan MJ, Allan LD. Intracardiac pressures in the human fetus. *Heart* 2000; **84**: 59–63.
15. Allan LD, Tynan MJ, Campbell S, Wilkinson JL, Anderson RH. Echocardiographic and anatomical correlates in the fetus. *Br Heart J* 1980; **44**: 444–451.
16. Espinoza J, Gotsch F, Kusanovic JP, Goncalves LF, Lee W, Hassan S, Mittal P, Schoen ML, Romero R. Changes in fetal cardiac geometry with gestation: implications for 3- and 4-dimensional fetal echocardiography. *J Ultrasound Med* 2007; **26**: 437–443; quiz 444.
17. Ahuja P, Sdek P, MacLellan WR. Cardiac myocyte cell cycle control in development, disease, and regeneration. *Physiol Rev* 2007; **87**: 521–544.
18. Saiki Y, Konig A, Waddell J, Rebeyka IM. Hemodynamic alteration by fetal surgery accelerates myocyte proliferation in fetal guinea pig hearts. *Surgery* 1997; **122**: 412–419.
19. Jonker SS, Zhang L, Louey S, Giraud GD, Thornburg KL, Faber JJ. Myocyte enlargement, differentiation, and proliferation kinetics in the fetal sheep heart. *J Appl Physiol* 2007; **102**: 1130–1142.
20. Chao G, Zheng C, Meng D, Su J, Xie X, Li W, Henein M. Tei index: the earliest detectable cardiac structural and functional abnormality detectable in Hb Bart's foetal edema. *Int J Cardiol* 2009; **134**: e150–154.
21. Godfrey M, Schimmel MS, Hammerman C, Farber B, Glaser J, Nir A. The incidence of congenital heart defects in very low birth weight and extremely low birth weight infants. *Isr Med Assoc J* 2010; **12**: 36–38.
22. Cui W, Roberson DA, Chen Z, Madronero LF, Cuneo BF. Systolic and diastolic time intervals measured from Doppler tissue imaging: normal values and Z-score tables, and effects of age, heart rate, and body surface area. *J Am Soc Echocardiogr* 2008; **21**: 361–370.
23. Pombo JF, Troy BL, Russell RO, Jr. Left ventricular volumes and ejection fraction by echocardiography. *Circulation* 1971; **43**: 480–490.
24. Allan LD, Joseph MC, Boyd EG, Campbell S, Tynan M. M-mode echocardiography in the developing human fetus. *Br Heart J* 1982; **47**: 573–583.
25. Quinones MA, Pickering E, Alexander JK. Percentage of shortening of the echocardiographic left ventricular dimension. Its use in determining ejection fraction and stroke volume. *Chest* 1978; **74**: 59–65.
26. DeVore GR. Assessing fetal cardiac ventricular function. *Semin Fetal Neonatal Med* 2005; **10**: 515–541.
27. Kjaergaard J, Akkan D, Iversen KK, Kober L, Torp-Pedersen C, Hassager C. Right ventricular dysfunction as an independent predictor of short- and long-term mortality in patients with heart failure. *Eur J Heart Fail* 2007; **9**: 610–616.
28. Carvalho JS, O'Sullivan C, Shinebourne EA, Henein MY. Right and left ventricular long-axis function in the fetus using angular M-mode. *Ultrasound Obstet Gynecol* 2001; **18**: 619–622.
29. Gardiner HM, Pasquini L, Wolfenden J, Barlow A, Li W, Kulinskaya E, Henein M. Myocardial tissue Doppler and long axis function in the fetal heart. *Int J Cardiol* 2006; **113**: 39–47.
30. Ho SY, Nihoyannopoulos P. Anatomy, echocardiography, and normal right ventricular dimensions. *Heart* 2006; **92** (Suppl 1): i2–13.
31. Abuhamad A, Chaoui R. Pulsed Doppler echocardiography. In *A practical guide to fetal echocardiography: Normal and abnormal hearts*. Lippincott, Williams, and Wilkins: Philadelphia, USA, 2009.
32. Fernandez Pineda L, Tamariz-Martel Moreno A, Maitre Azcarate MJ, Lopez Zea M, Rico Gomez F, Cazzaniga Bullon M, Quero Jimenez M. Contribution of Doppler atrioventricular flow waves to ventricular filling in the human fetus. *Pediatr Cardiol* 2000; **21**: 422–428.
33. Reed KL, Sahn DJ, Scagnelli S, Anderson CF, Shenker L. Doppler echocardiographic studies of diastolic function in the human fetal heart: changes during gestation. *J Am Coll Cardiol* 1986; **8**: 391–395.
34. Harada K, Rice MJ, Shiota T, Ishii M, McDonald RW, Reller MD, Sahn DJ. Gestational age- and growth-related alterations in fetal right and left ventricular diastolic filling patterns. *Am J Cardiol* 1997; **79**: 173–177.
35. Carceller-Blanchard AM, Fouron JC. Determinants of the Doppler flow velocity profile through the mitral valve of the human fetus. *Br Heart J* 1993; **70**: 457–460.
36. Chemla D, Coirault C, Hebert JL, Lecarpentier Y. Mechanics of Relaxation of the Human Heart. *News Physiol Sci* 2000; **15**: 78–83.
37. Baschat AA, Muench MV, Gembruch U. Coronary artery blood flow velocities in various fetal conditions. *Ultrasound Obstet Gynecol* 2003; **21**: 426–429.
38. Xie GY, Berk MR, Smith MD, Gurley JC, DeMaria AN. Prognostic value of Doppler transmitral flow patterns in patients with congestive heart failure. *J Am Coll Cardiol* 1994; **24**: 132–139.

39. Stirnemann JJ, Mougeot M, Proulx F, Nasr B, Essaoui M, Fouron JC, Ville Y. Profiling fetal cardiac function in twin-twin transfusion syndrome. *Ultrasound Obstet Gynecol* 2010; **35**: 19–27.
40. Mahle WT, Rychik J, Tian ZY, Cohen MS, Howell LJ, Crombleholme TM, Flake AW, Adzick NS. Echocardiographic evaluation of the fetus with congenital cystic adenomatoid malformation. *Ultrasound Obstet Gynecol* 2000; **16**: 620–624.
41. Crispi F, Hernandez-Andrade E, Pelsers MM, Plasencia W, Benavides-Serralde JA, Eixarch E, Le Noble F, Ahmed A, Glatz JF, Nicolaides KH, Gratacos E. Cardiac dysfunction and cell damage across clinical stages of severity in growth-restricted fetuses. *Am J Obstet Gynecol* 2008; **199**: 254 e251–258.
42. Choong CY, Herrmann HC, Weyman AE, Fifer MA. Preload dependence of Doppler-derived indexes of left ventricular diastolic function in humans. *J Am Coll Cardiol* 1987; **10**: 800–808.
43. Van Mieghem T, DeKoninck P, Steenhaut P, Deprest J. Methods for prenatal assessment of fetal cardiac function. *Prenat Diagn* 2009; **29**: 1193–1203.
44. Hecher K, Campbell S, Doyle P, Harrington K, Nicolaides K. Assessment of fetal compromise by Doppler ultrasound investigation of the fetal circulation. Arterial, intracardiac, and venous blood flow velocity studies. *Circulation* 1995; **91**: 129–138.
45. Makikallio K, McElhinney DB, Levine JC, Marx GR, Colan SD, Marshall AC, Lock JE, Marcus EN, Tworetzky W. Fetal aortic valve stenosis and the evolution of hypoplastic left heart syndrome: patient selection for fetal intervention. *Circulation* 2006; **113**: 1401–1405.
46. Rychik J, Tian Z, Bebbington M, Xu F, McCann M, Mann S, Wilson RD, Johnson MP. The twin-twin transfusion syndrome: spectrum of cardiovascular abnormality and development of a cardiovascular score to assess severity of disease. *Am J Obstet Gynecol* 2007; **197**: 392 e391–398.
47. Makikallio K, Rasanen J, Makikallio T, Vuolteenaho O, Huhta JC. Human fetal cardiovascular profile score and neonatal outcome in intrauterine growth restriction. *Ultrasound Obstet Gynecol* 2008; **31**: 48–54.
48. Mori Y, Rice MJ, McDonald RW, Reller MD, Wanitkun S, Harada K, Sahn DJ. Evaluation of systolic and diastolic ventricular performance of the right ventricle in fetuses with ductal constriction using the Doppler Tei index. *Am J Cardiol* 2001; **88**: 1173–1178.
49. Tei C, Ling LH, Hodge DO, Bailey KR, Oh JK, Rodeheffer RJ, Tajik AJ, Seward JB. New index of combined systolic and diastolic myocardial performance: a simple and reproducible measure of cardiac function–a study in normals and dilated cardiomyopathy. *J Cardiol* 1995; **26**: 357–366.
50. Friedman D, Buyon J, Kim M, Glickstein JS. Fetal cardiac function assessed by Doppler myocardial performance index (Tei Index). *Ultrasound Obstet Gynecol* 2003; **21**: 33–36.
51. Pellett AA, Tolar WG, Merwin DG, Kerut EK. The Tei index: methodology and disease state values. *Echocardiography* 2004; **21**: 669–672.
52. Tsutsumi T, Ishii M, Eto G, Hota M, Kato H. Serial evaluation for myocardial performance in fetuses and neonates using a new Doppler index. *Pediatr Int* 1999; **41**: 722–727.
53. Hernandez-Andrade E, Lopez-Tenorio J, Figueroa-Diesel H, Sanin-Blair J, Carreras E, Cabero L, Gratacos E. A modified myocardial performance (Tei) index based on the use of valve clicks improves reproducibility of fetal left cardiac function assessment. *Ultrasound Obstet Gynecol* 2005; **26**: 227–232.
54. Hernandez-Andrade E, Figueroa-Diesel H, Kottman C, Illanes S, Arraztoa J, Acosta-Rojas R, Gratacos E. Gestational-age-adjusted reference values for the modified myocardial performance index for evaluation of fetal left cardiac function. *Ultrasound Obstet Gynecol* 2007; **29**: 321–325.
55. van Splunder IP, Wladimiroff JW. Cardiac functional changes in the human fetus in the late first and early second trimesters. *Ultrasound Obstet Gynecol* 1996; **7**: 411–415.
56. Van Mieghem T, Gucciardo L, Lewi P, Lewi L, Van Schoubroeck D, Devlieger R, De Catte L, Verhaeghe J, Deprest J. Validation of the fetal myocardial performance index in the second and third trimesters of gestation. *Ultrasound Obstet Gynecol* 2009; **33**: 58–63.
57. Duan Y, Harada K, Wu W, Ishii H, Takada G. Correlation between right ventricular Tei index by tissue Doppler imaging and pulsed Doppler imaging in fetuses. *Pediatr Cardiol* 2008; **29**: 739–743.
58. Tekten T, Onbasili AO, Ceyhan C, Unal S, Discigil B. Novel approach to measure myocardial performance index: pulsed-wave tissue Doppler echocardiography. *Echocardiography* 2003; **20**: 503–510.
59. Rojo EC, Rodrigo JL, Perez de Isla L, Almeria C, Gonzalo N, Aubele A, Cinza R, Zamorano J, Macaya C. Disagreement between tissue Doppler imaging and conventional pulsed wave Doppler in the measurement of myocardial performance index. *Eur J Echocardiogr* 2006; **7**: 356–364.
60. Raboisson MJ, Fouron JC, Lamoureux J, Leduc L, Grignon A, Proulx F, Gamache S. Early intertwin differences in myocardial performance during the twin-to-twin transfusion syndrome. *Circulation* 2004; **110**: 3043–3048.
61. Letti Muller AL, Barrios Pde M, Kliemann LM, Valerio EG, Gasnier R, Magalhaes JA. Tei index to assess fetal cardiac performance in fetuses at risk for fetal inflammatory response syndrome. *Ultrasound Obstet Gynecol* 2010; **36**: 26–31.
62. Ichizuka K, Matsuoka R, Hasegawa J, Shirato N, Jimbo M, Otsuki K, Sekizawa A, Farina A, Okai T. The Tei index for evaluation of fetal myocardial performance in sick fetuses. *Early Hum Dev* 2005; **81**: 273–279.
63. Cruz-Martinez R, Figueras F, Jaramillo JJ, Meler E, Mendez A, Hernandez-Andrade E, Gratacos E. Learning curve for Doppler measurement of fetal modified myocardial performance index. *Ultrasound Obstet Gynecol* 2011; **37**: 158–162.
64. Sud S, Massel D. An echocardiographic study of the limitations of the Tei index in aortic stenosis. *Echocardiography* 2009; **26**: 891–899.
65. Mohrman DE, Heller LJ. The heart pump. In *Cardiovascular Physiology*. McGraw-Hill: USA, 2010; Chapter 3.
66. Dyer KL, Pauliks LB, Das B, Shandas R, Ivy D, Shaffer EM, Valdes-Cruz LM. Use of myocardial performance index in pediatric patients with idiopathic pulmonary arterial hypertension. *J Am Soc Echocardiogr* 2006; **19**: 21–27.
67. Gutgesell HP. Novel index relating both isovolumetric contraction time and isovolumetric relaxation time to ejection time. *J Am Soc Echocardiogr* 1997; **10**: 781–782.
68. Cheung MM, Smallhorn JF, Redington AN, Vogel M. The effects of changes in loading conditions and modulation of inotropic state on the myocardial performance index: comparison with conductance catheter measurements. *Eur Heart J* 2004; **25**: 2238–2242.
69. Eidem BW, O'Leary PW, Tei C, Seward JB. Usefulness of the myocardial performance index for assessing right ventricular function in congenital heart disease. *Am J Cardiol* 2000; **86**: 654–658.
70. Yagel S, Cohen SM, Shapiro I, Valsky DV. 3D and 4D ultrasound in fetal cardiac scanning: a new look at the fetal heart. *Ultrasound Obstet Gynecol* 2007; **29**: 81–95.
71. Yagel S, Cohen SM, Achiron R. Examination of the fetal heart by five short-axis views: a proposed screening method for comprehensive cardiac evaluation. *Ultrasound Obstet Gynecol* 2001; **17**: 367–369.
72. Esh-Broder E, Ushakov FB, Imbar T, Yagel S. Application of free-hand three-dimensional echocardiography in the evaluation of fetal cardiac ejection fraction: a preliminary study. *Ultrasound Obstet Gynecol* 2004; **23**: 546–551.
73. Messing B, Cohen SM, Valsky DV, Rosenak D, Hochner-Celnikier D, Savchev S, Yagel S. Fetal cardiac ventricle

volumetry in the second half of gestation assessed by 4D ultrasound using STIC combined with inversion mode. *Ultrasound Obstet Gynecol* 2007; **30**: 142–151.
74. Molina FS, Faro C, Sotiriadis A, Dagklis T, Nicolaides KH. Heart stroke volume and cardiac output by four-dimensional ultrasound in normal fetuses. *Ultrasound Obstet Gynecol* 2008; **32**: 181–187.
75. Uittenbogaard LB, Haak MC, Spreeuwenberg MD, van Vugt JM. Fetal cardiac function assessed with four-dimensional ultrasound imaging using spatiotemporal image correlation. *Ultrasound Obstet Gynecol* 2009; **33**: 272–281.
76. Rizzo G, Capponi A, Cavicchioni O, Vendola M, Arduini D. Fetal cardiac stroke volume determination by four-dimensional ultrasound with spatio-temporal image correlation compared with two-dimensional and Doppler ultrasonography. *Prenat Diagn* 2007; **27**: 1147–1150.
77. Kusanovic JP, Nien JK, Goncalves LF, Espinoza J, Lee W, Balasubramaniam M, Soto E, Erez O, Romero R. The use of inversion mode and 3D manual segmentation in volume measurement of fetal fluid-filled structures: comparison with Virtual Organ Computer-aided AnaLysis (VOCAL). *Ultrasound Obstet Gynecol* 2008; **31**: 177–186.
78. Hamill N, Romero R, Hassan SS, Lee W, Myers SA, Mittal P, Kusanovic JP, Chaiworapongsa T, Vaisbuch E, Espinoza J, Gotsch F, Carletti A, Goncalves LF, Yeo L. Repeatability and reproducibility of fetal cardiac ventricular volume calculations using spatiotemporal image correlation and virtual organ computer-aided analysis. *J Ultrasound Med* 2009; **28**: 1301–1311.
79. Myerson MH, Montgomery HE, World MJ, Pennell DJ. Left ventricular mass: reliability of M-mode and 2-dimensional echocardiographic formulas. *Hypertension* 2002; **40**: 673–678.
80. Messing B, Valsky DV, Rosenak D, Cohen SM, Yagel S. 3D/4D ultrasound for fetal cardiac ventricle mass measurement in the second half of gestation in normal and anomalous cases. *Ultrasound Obstet Gynecol* 2008; **32**: 335.
81. Ho CY, Solomon SD. A clinician's guide to tissue Doppler imaging. *Circulation* 2006; **113**: e396–398.
82. McCulloch M, Zoghbi WA, Davis R, Thomas C, Dokainish H. Color tissue Doppler myocardial velocities consistently underestimate spectral tissue Doppler velocities: impact on calculation peak transmitral pulsed Doppler velocity/early diastolic tissue Doppler velocity (E/Ea). *J Am Soc Echocardiogr* 2006; **19**: 744–748.
83. Park YS, Park JH, Ahn KT, Jang WI, Park HS, Kim JH, Lee JH, Choi SW, Jeong JO, Seong IW. Usefulness of mitral annular systolic velocity in the detection of left ventricular systolic dysfunction: comparison with three dimensional echocardiographic data. *J Cardiovasc Ultrasound* 2010; **18**: 1–5.
84. Derumeaux G, Ovize M, Loufoua J, Andre-Fouet X, Minaire Y, Cribier A, Letac B. Doppler tissue imaging quantitates regional wall motion during myocardial ischemia and reperfusion. *Circulation* 1998; **97**: 1970–1977.
85. Sohn DW, Chai IH, Lee DJ, Kim HC, Kim HS, Oh BH, Lee MM, Park YB, Choi YS, Seo JD, Lee YW. Assessment of mitral annulus velocity by Doppler tissue imaging in the evaluation of left ventricular diastolic function. *J Am Coll Cardiol* 1997; **30**: 474–480.
86. Ommen SR, Nishimura RA, Appleton CP, Miller FA, Oh JK, Redfield MM, Tajik AJ. Clinical utility of Doppler echocardiography and tissue Doppler imaging in the estimation of left ventricular filling pressures: A comparative simultaneous Doppler-catheterization study. *Circulation* 2000; **102**: 1788–1794.
87. Yu CM, Fung JW, Zhang Q, Kum LC, Lin H, Yip GW, Wang M, Sanderson JE. Tissue Doppler echocardiographic evidence of atrial mechanical dysfunction in coronary artery disease. *Int J Cardiol* 2005; **105**: 178–185.
88. Harada K, Tsuda A, Orino T, Tanaka T, Takada G. Tissue Doppler imaging in the normal fetus. *Int J Cardiol* 1999; **71**: 227–234.
89. Aoki M, Harada K, Ogawa M, Tanaka T. Quantitative assessment of right ventricular function using doppler tissue imaging in fetuses with and without heart failure. *J Am Soc Echocardiogr* 2004; **17**: 28–35.
90. Watanabe S, Hashimoto I, Saito K, Watanabe K, Hirono K, Uese K, Ichida F, Saito S, Miyawaki T, Niemann P, Sahn DJ. Characterization of ventricular myocardial performance in the fetus by tissue Doppler imaging. *Circ J* 2009; **73**: 943–947.
91. Comas M, Crispi F, Cruz-Martinez R, Martinez JM, Figueras F, Gratacos E. Usefulness of myocardial tissue Doppler vs conventional echocardiography in the evaluation of cardiac dysfunction in early-onset intrauterine growth restriction. *Am J Obstet Gynecol* 2010; **203**: 45 e41–47.
92. Barker PC, Houle H, Li JS, Miller S, Herlong JR, Camitta MG. Global longitudinal cardiac strain and strain rate for assessment of fetal cardiac function: novel experience with velocity vector imaging. *Echocardiography* 2009; **26**: 28–36.
93. Pellerin D, Sharma R, Elliott P, Veyrat C. Tissue Doppler, strain, and strain rate echocardiography for the assessment of left and right systolic ventricular function. *Heart* 2003; **89** (Suppl 3): iii9–17.
94. Perk G, Tunick PA, Kronzon I. Non-Doppler two-dimensional strain imaging by echocardiography–from technical considerations to clinical applications. *J Am Soc Echocardiogr* 2007; **20**: 234–243.
95. Blessberger H, Binder T. NON-invasive imaging: Two dimensional speckle tracking echocardiography: basic principles. *Heart* 2010; **96**: 716–722.
96. Simpson J. Speckle tracking for the assessment of fetal cardiac function. *Ultrasound Obstet Gynecol* 2011; **37**: 133–134.
97. Matsui H, Germanakis I, Kulinskaya E, Gardiner HM. Temporal and spatial performance of vector velocity imaging in the human fetal heart. *Ultrasound Obstet Gynecol* 2011; **37**: 150–157.
98. Nagueh SF, Appleton CP, Gillebert TC, Marino PN, Oh JK, Smiseth OA, Waggoner AD, Flachskampf FA, Pellikka PA, Evangelisa A. Recommendations for the evaluation of left ventricular diastolic function by echocardiography. *Eur J Echocardiogr* 2009; **10**: 165–193.
99. Reichek N. Magnetic resonance imaging for assessment of myocardial function. *Magn Reson Q* 1991; **7**: 255–274.
100. Mogelvang J, Stubgaard M, Thomsen C, Henriksen O. Evaluation of right ventricular volumes measured by magnetic resonance imaging. *Eur Heart J* 1988; **9**: 529–533.
101. Krishnamurthy R. The role of MRI and CT in congenital heart disease. *Pediatr Radiol* 2009; **39** (Suppl 2): S196–204.
102. Gorincour G, Bourliere-Najean B, Bonello B, Fraisse A, Philip N, Potier A, Kreitmann B, Petit P. Feasibility of fetal cardiac magnetic resonance imaging: preliminary experience. *Ultrasound Obstet Gynecol* 2007; **29**: 105–108.
103. Saleem SN. Feasibility of MRI of the fetal heart with balanced steady-state free precession sequence along fetal body and cardiac planes. *AJR Am J Roentgenol* 2008; **191**: 1208–1215.
104. Fogel MA, Wilson RD, Flake A, Johnson M, Cohen D, McNeal G, Tian ZY, Rychik J. Preliminary investigations into a new method of functional assessment of the fetal heart using a novel application of 'real-time' cardiac magnetic resonance imaging. *Fetal Diagn Ther* 2005; **20**: 475–480.
105. Meyer-Wittkopf M, Cook A, McLennan A, Summers P, Sharland GK, Maxwell DJ. Evaluation of three-dimensional ultrasonography and magnetic resonance imaging in assessment of congenital heart anomalies in fetal cardiac specimens. *Ultrasound Obstet Gynecol* 1996; **8**: 303–308.
106. Ertl-Wagner B, Lienemann A, Strauss A, Reiser MF. Fetal magnetic resonance imaging: indications, technique, anatomical considerations and a review of fetal abnormalities. *Eur Radiol* 2002; **12**: 1931–1940.

107. Holmes WM, McCabe C, Mullin JM, Condon B, Bain MM. Images in cardiovascular medicine. Noninvasive self-gated magnetic resonance cardiac imaging of developing chick embryos in ovo. *Circulation* 2008; **117**: e346–347.
108. Rizzo G, Arduini D, Romanini C. Umbilical vein pulsations: a physiologic finding in early gestation. *Am J Obstet Gynecol* 1992; **167**: 675–677.
109. Baschat AA, Harman CR. Venous Doppler in the assessment of fetal cardiovascular status. *Curr Opin Obstet Gynecol* 2006; **18**: 156–163.
110. Maiz N, Valencia C, Emmanuel EE, Staboulidou I, Nicolaides KH. Screening for adverse pregnancy outcome by ductus venosus Doppler at 11–13+6 weeks of gestation. *Obstet Gynecol* 2008; **112**: 598–605.
111. Quintero RA, Morales WJ, Allen MH, Bornick PW, Johnson PK, Kruger M. Staging of twin-twin transfusion syndrome. *J Perinatol* 1999; **19**: 550–555.
112. Nakai Y, Miyazaki Y, Matsuoka Y, Matsumoto M, Imanaka M, Ogita S. Pulsatile umbilical venous flow and its clinical significance. *Br J Obstet Gynaecol* 1992; **99**: 977–980.
113. Turan OM, Turan S, Gungor S, Berg C, Moyano D, Gembruch U, Nicolaides KH, Harman CR, Baschat AA. Progression of Doppler abnormalities in intrauterine growth restriction. *Ultrasound Obstet Gynecol* 2008; **32**: 160–167.
114. Makikallio K, Vuolteenaho O, Jouppila P, Rasanen J. Association of severe placental insufficiency and systemic venous pressure rise in the fetus with increased neonatal cardiac troponin T levels. *Am J Obstet Gynecol* 2000; **183**: 726–731.
115. Makikallio K, Vuolteenaho O, Jouppila P, Rasanen J. Ultrasonographic and biochemical markers of human fetal cardiac dysfunction in placental insufficiency. *Circulation* 2002; **105**: 2058–2063.
116. Girsen A, Ala-Kopsala M, Makikallio K, Vuolteenaho O, Rasanen J. Cardiovascular hemodynamics and umbilical artery N-terminal peptide of proB-type natriuretic peptide in human fetuses with growth restriction. *Ultrasound Obstet Gynecol* 2007; **29**: 296–303.
117. Mori A, Trudinger B, Mori R, Reed V, Takeda Y. The fetal central venous pressure waveform in normal pregnancy and in umbilical placental insufficiency. *Am J Obstet Gynecol* 1995; **172**: 51–57.
118. Mori A, Uchida N, Ishiguro Y, Atsuko T, Kanako M, Mikio M. Evaluation of cardiac function of the fetus by inferior vena cava diameter pulse waveform. *Am Heart J* 2007; **154**: 789–794.
119. Hecher K, Hackeloer BJ. Cardiotocogram compared to Doppler investigation of the fetal circulation in the premature growth-retarded fetus: longitudinal observations. *Ultrasound Obstet Gynecol* 1997; **9**: 152–161.
120. Baschat AA, Gembruch U, Harman CR. The sequence of changes in Doppler and biophysical parameters as severe fetal growth restriction worsens. *Ultrasound Obstet Gynecol* 2001; **18**: 571–577.
121. Alberry M, Soothill P. Management of fetal growth restriction. *Arch Dis Child Fetal Neonatal Ed* 2007; **92**: F62–67.
122. Yagel S, Valsky DV. From anatomy to function: the developing image of ultrasound evaluation. *Ultrasound Obstet Gynecol* 2008; **31**: 615–617.
123. Yagel S, Kivilevitch Z, Cohen SM, Valsky DV, Messing B, Shen O, Achiron R. The fetal venous system, part I: normal embryology, anatomy, hemodynamics, ultrasound evaluation and Doppler investigation. *Ultrasound Obstet Gynecol* 2010; **35**: 741–750.
124. Yagel S, Kivilevitch Z, Cohen SM, Valsky DV, Messing B, Shen O, Achiron R. The fetal venous system, Part II: ultrasound evaluation of the fetus with congenital venous system malformation or developing circulatory compromise. *Ultrasound Obstet Gynecol* 2010; **36**: 93–111.

